

Mechanism of proton- ^3He elastic backward scattering at intermediate energy

A.P. Kobushkin,* E.A. Stokovskiy,[†] and K. Hatanaka[‡]
*Research Center for Nuclear Physics, Osaka University,
10-1 Mihogaoka, Ibaraki, Osaka, 567-0047, Japan*

S. Ishikawa

Hosei University, Department of Physics, Fujimi 2-17-1, Chiyoda, Tokyo, 102-8160, Japan
(Dated: December 14, 2018)

We provide systematic analysis of the proton- ^3He elastic scattering at $\theta_{\text{cm}} = 180^\circ$ and at the incident proton energy $T_p \lesssim 700$ MeV. Three mechanisms are discussed: 2N pair exchange in the triplet and singlet spin states, pion-exchange and direct mechanism. It is shown that at $T_p \gtrsim 150$ MeV three-body structure, including triplet and singlet scattering states of the 2N pair, becomes of great importance for understanding energy dependence of the reaction observables. Predictions for the differential cross section and the polarization correlation C_{00nn} which can be studied now in experiment are given.

PACS numbers: 21.30.Cb, 21.30.-x, 25.40.Cm, 25.55.c

I. INTRODUCTION

For several decades considerable efforts have been done to investigate structure of the lightest nuclei (the deuteron, ^3He , ^4He) at short distances between the constituent nucleons. Significant progress was achieved both in theory and experiment, first of all because high quality data on spin-dependent observables were obtained with both hadronic [1, 2] and electromagnetic probes [3]. Large part of these investigations consists of study of elastic backward (in the center of mass system) proton – nucleus scattering (EBS). This process involves large momentum transfer $|t|$ and therefore a belief exists that EBS can provide an access to the high momentum components of the wave function of the lightest nuclei.

From those investigations it becomes obvious that at present there is no theoretical model which quantitatively describes the existing data, even for the simplest reaction, pd EBS (see [2] and Refs. therein). Surprisingly, the wide gap exists between precise and detailed data base and rather imprecise (even qualitatively) theoretical understanding of these reactions.

The elastic backward $p(^3\text{He}, p)^3\text{He}$ scattering is studied in much less detail than the pd EBS. But presently, high intensity beams of polarized protons in combination with polarized ^3He targets [4] give an opportunity to perform detailed studies of $p^3\text{He}$ EBS with spin dependent observables at energy between 200 to 400 MeV [5]. This, in turn, demands careful theoretical study of the reaction mechanism, specially at intermediate energy.

The goal of the present study is to develop a theoretical description of the proton EBS off the lightest nuclei, which provides predictions for experimentally measurable observables including spin-dependent ones. In the present paper the $p^3\text{He}$ EBS up to $T_p \sim 0.7$ GeV is considered only. In this particular case a request from experiment is to find an adequate connection of this reaction with the structure of the 3N system and to get quantitative estimations for sensitivities of its cross section and spin-dependent observables to the existing wave functions of ^3He .

The mechanism of one-deuteron-exchange shows that such connection exists, but it fails to reproduce cross section data at $T_p > 200$ MeV [6]. The exchange of the singlet spin np pair, in addition to the one-deuteron-exchange, also does not explain existing data at intermediate energy [7]. In the present paper we take into account full three-body structure of ^3He and consider 2N-exchange in the singlet and the triplet spin states (the upper-left diagram of Figure 1). Note that the one-deuteron-exchange gives only a partial contribution in the triplet 2N-exchange.

It was stressed by many authors that the so-called pion (PI) mechanism is responsible for the “shoulder” in the measured energy dependence of the differential cross section of $p^3\text{He}$ EBS between 200 and 700 MeV [8]-[10]. Following the general ideas coming from the similar situation in pd -EBS [11, 12], the authors of Refs.[8]-[10] estimated the contribution of PI-mechanism from the triangle diagram with subprocesses $pd \rightarrow ^3\text{He}\pi^0$, $pd^* \rightarrow ^3\text{He}\pi$. However, it was already mentioned that in the triangle diagram the initial and the final nuclei are coupled in different vertices and thus this diagram is not T-invariant [13]. Moreover, sometimes it is difficult to avoid double-counting with other mechanisms in such approach.

We estimate PI-mechanism from a two-loop diagram where high momentum from the initial to the final proton is transferred by a virtual pion scattered off the intermediate deuteron (the upper-right diagram of Figure 1).

*Also at Bogolyubov Institute for Theoretical Physics, Metrologicheskaya str. 14B, 03143 Kiev, Ukraine; Electronic address: akob@rcnp.osaka-u.ac.jp

[†]Also at LPP, Joint Institute for Nuclear Research, 141980, Dubna, Moscow region, Russia; Electronic address: strok@rcnp.osaka-u.ac.jp

[‡]Electronic address: hatanaka@rcnp.osaka-u.ac.jp

For the backward pd scattering similar mechanism (elastic πN scattering in the region of Δ -resonance) was discussed in [14]. We use results of the partial wave analysis of the elastic πd scattering done by Virginia group [15], what makes not necessary to take into account resonance propagator explicitly. Some authors propose another way to consider pion degrees of freedom which also does not contain the abovementioned difficulties [16]. In our case it corresponds to the bottom-left diagram of Figure 1. Kinematic estimations show that this diagram may contribute significantly near $T_p \sim 0.5$ GeV and thus it is not essential at RCNP energy. Alternatively the main contribution of the upper-right diagram of Figure 1 appears earlier, around $T_p \sim 0.3$ GeV, exactly at the energy of the experiment [5]. It corresponds to the pion energy $T_\pi \approx 0.2$ GeV, where the differential cross section of the elastic πd scattering has a sharp resonance-like structure [17].

Among other important mechanisms, the so-called direct mechanism (DIR, the bottom-right diagram of Figure 1) may also play important role in this reaction [9, 18].

The paper is organized as follows. In Sec. II the general formalism of the reaction is given. Parametrization for the ${}^3\text{He}$ wave function is discussed in Sec. III. In the same section we give also results for two-nucleon momentum distributions and densities in singlet and triplet spin states coming from this parametrization. Then, in Sec. IV, we derive reaction amplitudes for three mechanisms, 2N-exchange, PI and DIR. Results of numerical calculations, comparison with experiment and predictions are presented in Sec. V. Conclusions and remarks are given in Sec. VI.

II. GENERAL FORMALISM

Parity and time-reversal invariance leaves only 6 independent complex amplitudes for the elastic scattering of two spin- $\frac{1}{2}$ particles. At $\theta_{\text{cm}} = 180^\circ$ three of them vanish and they are reduced to

$$\begin{aligned} \mathcal{M}(\theta_{\text{cm}} = 180^\circ) &= \begin{pmatrix} \mathcal{M}_{++}^{++} & \mathcal{M}_{+-}^{++} & \mathcal{M}_{-+}^{++} & \mathcal{M}_{--}^{++} \\ \mathcal{M}_{++}^{+-} & \mathcal{M}_{+-}^{+-} & \mathcal{M}_{-+}^{+-} & \mathcal{M}_{--}^{+-} \\ \mathcal{M}_{++}^{-+} & \mathcal{M}_{+-}^{-+} & \mathcal{M}_{-+}^{-+} & \mathcal{M}_{--}^{-+} \\ \mathcal{M}_{++}^{--} & \mathcal{M}_{+-}^{--} & \mathcal{M}_{-+}^{--} & \mathcal{M}_{--}^{--} \end{pmatrix} \\ &= \begin{pmatrix} A & 0 & 0 & 0 \\ 0 & F & G & 0 \\ 0 & G & F & 0 \\ 0 & 0 & 0 & A \end{pmatrix} \end{aligned} \quad (1)$$

Here $\mathcal{M}_{Mm}^{M'm'}$ is amplitude with M , m and M' , m' magnetic quantum numbers of ${}^3\text{He}$ and the proton in initial and final states, respectively. We assume the normalization when the differential cross section is given by

$$\frac{d\sigma}{d\Omega_{\text{cm}}} = \frac{\frac{1}{4}\text{Tr}(\mathcal{M}\mathcal{M}^\dagger)}{64\pi^2 s} = \frac{|A|^2 + |F|^2 + |G|^2}{128\pi^2 s}, \quad (2)$$

where s is the total c.m. energy squared and the factor $\frac{1}{4}$ comes from the average over the initial spin states.

Corresponding to the three non-vanishing amplitudes there are $2 \times 3 - 1 = 5$ independent observables: the differential cross section (2) and 4 spin-dependent observables. Among the last ones we will consider in this paper only polarization correlation

$$C_{00nn} = \frac{\text{Tr}(\mathcal{M}\sigma_y(\text{He})\mathcal{M}^\dagger\sigma_y(p))}{\text{Tr}(\mathcal{M}\mathcal{M}^\dagger)} = \frac{2\text{Re}(AG^*)}{|A|^2 + |F|^2 + |G|^2}. \quad (3)$$

III. ${}^3\text{He}$ WAVE FUNCTION

In forthcoming calculations we use a new parametrization of full antisymmetric trinucleon wave function (TWF) [19] for Paris [20] and CD-Bonn [21] potentials. It is restricted by the five partial wave components

$$\nu = \{ {}^1s_0S, {}^3s_1S, {}^3s_1D, {}^3d_1S, {}^3s_1D \}, \quad (4)$$

where 1s_0 etc. correspond to a pair of nucleons and S and D denotes relative angular momentum between the pair and the spectator nucleon. The components for higher angular momenta were shown to be insignificant. The (1,2) pair is chosen as an active pair and the TWF components are defined as follows

$$\begin{aligned} \langle r\rho\nu|\Psi\rangle &= \langle r\rho\nu|\psi[(12)3]\rangle \\ &+ \sum_{\nu_{23}} \langle r\rho\nu|\psi[(23)1]\rangle + \sum_{\nu_{31}} \langle r\rho\nu|\psi[(31)2]\rangle, \end{aligned} \quad (5)$$

where

$$\langle r\rho\nu|\Psi\rangle = \sum \langle \dots \rangle Y_{l_3}(\hat{r}) Y_{LL_3}(\hat{\rho}) \Psi_\nu(r, \rho) \quad (6)$$

and $\langle \dots \rangle$ denotes all necessary spin and isospin Clebsch-Gordan coefficients; $\vec{r} = \vec{r}_{12}$ is the relative coordinate in the pair and $\vec{\rho} = \vec{\rho}_3$ is the relative coordinate between the pair center of mass and the third nucleon. In the momentum space \vec{p} and \vec{q} are used for the relative momentum in the pair and the relative momentum between the pair and the third nucleon, respectively.

The normalization is given by

$$\int_0^\infty dr d\rho \sum_\nu |\Psi_\nu(r, \rho)|^2 = 1. \quad (7)$$

Important quantities in our calculations are momentum distributions of a virtual (np) pair in triplet ($j = 1$) and

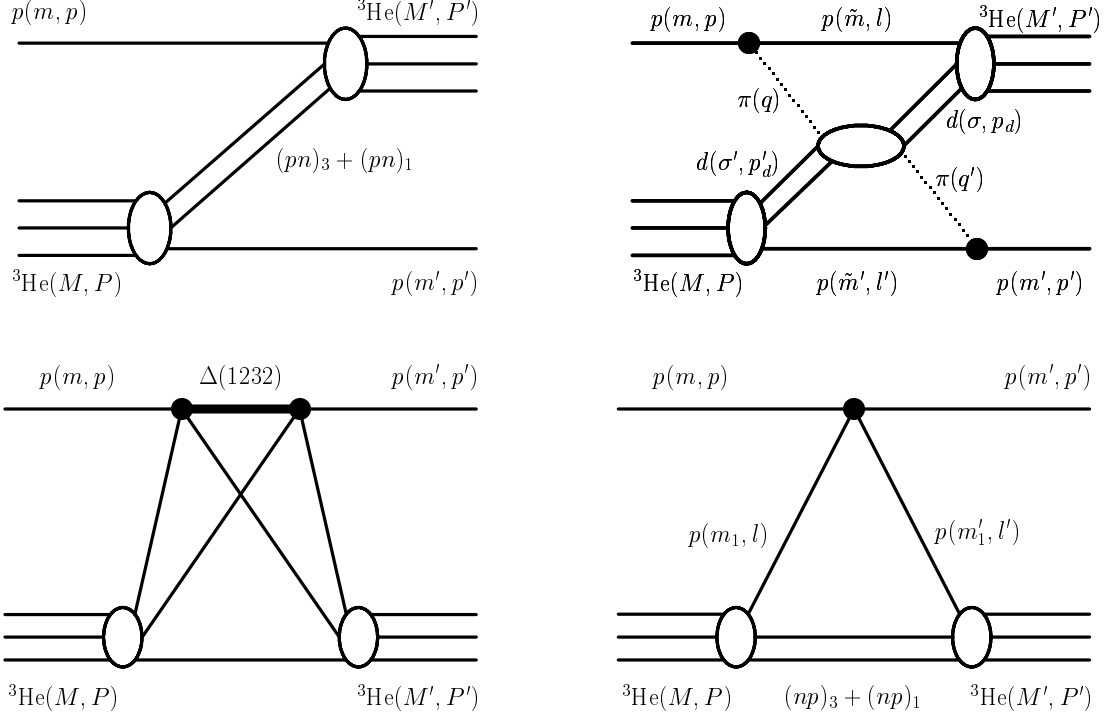


FIG. 1: Mechanisms of the proton- ^3He backward scattering at intermediate energy: 2N-exchange (upper-left diagram), PI (upper-right diagram), the Δ -excitation (bottom-left diagram) and DIR (bottom-right diagram).

singlet ($j = 0$) states

$$\begin{aligned}
 n_3^S(q) &= 3 \int_0^\infty dp p^2 \left[|\Psi_{3s_1S}(p, q)|^2 + |\Psi_{3d_1S}(p, q)|^2 \right], \\
 n_3^D(q) &= 3 \int_0^\infty dp p^2 \left[|\Psi_{3s_1D}(p, q)|^2 + |\Psi_{3d_1D}(p, q)|^2 \right], \\
 n_3^{\text{int}}(q) &= 3 \int_0^\infty dp p^2 \left[\Psi_{3s_1S}(p, q) \Psi_{3s_1D}(p, q) \right. \\
 &\quad \left. + \Psi_{3d_1S}(p, q) \Psi_{3d_1D}(p, q) \right], \\
 n_1(q) &= 3 \int_0^\infty dp p^2 |\Psi_{1s_0S}(p, q)|^2, \quad (8)
 \end{aligned}$$

where the factor 3 is a combinatorial factor and the bottom suffix is $2j + 1$.

For PI-mechanism we also need the deuteron momentum distribution in ^3He . It is given by the S and D waves for relative motion in the $d + p$ -component of the ^3He wave function

$$\begin{aligned}
 u(q) &= \int_0^\infty dp p^2 \left[u_d(p) \Psi_{3s_1S}(p, q) + \right. \\
 &\quad \left. + w_d(p) \Psi_{3d_1S}(p, q) \right], \\
 w(q) &= \int_0^\infty dp p^2 \left[u_d(p) \Psi_{3s_1D}(p, q) + \right. \\
 &\quad \left. + w_d(p) \Psi_{3d_1D}(p, q) \right], \quad (9)
 \end{aligned}$$

where $u_d(p)$ and $w_d(p)$ are the deuteron S and D wave functions, respectively. Now the deuteron momentum distribution reads

$$n_d(q) = n_d^S(q) + n_d^D(q) = 3 [u^2(q) + w^2(q)], \quad (10)$$

where $n_d^S(q) = 3u^2(q)$ and $n_d^D(q) = 3w^2(q)$ have meaning of the deuteron momentum distributions in the S and D waves. Partially they contribute to $n_3^S(q)$ and $n_3^D(q)$, respectively. The quantity $n_d^{\text{int}}(q) = 3u(q)w(q)$ corresponds to the deuteron contribution in the “interference” momentum distribution $n_3^{\text{int}}(q)$.

According to the normalization (7) the quantity

$$\begin{aligned}
 N_d &= \int_0^\infty dq q^2 (n_d^S(q) + n_d^D(q)) \\
 &= 3 \int_0^\infty dq q^2 [u^2(q) + w^2(q)] \quad (11)
 \end{aligned}$$

has meaning of the effective number of the deuterons in ^3He . We obtain $N_d = 1.39$ for Paris potential and $N_d = 1.36$ for CD-Bonn potential. This agrees well with $N_d = 1.38$ obtained earlier for Urbana and Argonne potentials [22].

In Figure 2 the momentum distributions of the triplet pair in S and D waves are compared with that for the

deuteron in ${}^3\text{He}$. The interference momentum distribution and the momentum distribution of the singlet pair are displayed in Figure 3 and 4, respectively.

From Figures 2 and 3 one learns that at internal momentum $q < 300$ MeV/c the triplet two-body pair exists mainly as real deuteron, but at higher q the contribution of nonbound (np) pair becomes essential.

Appropriate two-body densities in configuration space

$$\begin{aligned}\rho_3^S(\rho) &= 3 \int_0^\infty dr \left[|\Psi_{3s_1S}(r, \rho)|^2 + |\Psi_{3d_1S}(r, \rho)|^2 \right], \\ \rho_3^D(\rho) &= 3 \int_0^\infty dr \left[|\Psi_{3s_1D}(r, \rho)|^2 + |\Psi_{3d_1D}(r, \rho)|^2 \right], \\ \rho_3^{\text{int}}(\rho) &= 3 \int_0^\infty dr \left[\Psi_{3s_1S}(r, \rho)\Psi_{3s_1D}(r, \rho) + \Psi_{3d_1S}(r, \rho)\Psi_{3d_1D}(r, \rho) \right], \\ \rho_1(\rho) &= 3 \int_0^\infty dr |\Psi_{1s_0S}(r, \rho)|^2\end{aligned}\quad (12)$$

are shown in Figures 5 and 6. The triplet densities are also compared with densities for the deuteron in ${}^3\text{He}$.

IV. DERIVATION OF REACTION AMPLITUDE

A. 2N-exchange

In the nonrelativistic limit and at $\theta_{\text{cm}} = 180^\circ$ the corresponding amplitudes $A^{(2N)}$, $F^{(2N)}$ and $G^{(2N)}$ of (1) read (see, e.g., [7])

$$\begin{aligned}A^{(2N)} &= \frac{1}{3}t_3 \left[n_3^S(k) - 2\sqrt{2}n_3^{\text{int}}(k) + 2n_3^D(k) \right] \\ &\quad + \frac{1}{3}t_1n_1(k), \\ F^{(2N)} &= \frac{1}{3}t_3 \left[2n_3^S(k) + 2\sqrt{2}n_3^{\text{int}}(k) + n_3^D(k) \right], \\ G^{(2N)} &= \frac{1}{3}t_3 \left[-n_3^S(k) + 2\sqrt{2}n_3^{\text{int}}(k) - 2n_3^D(k) \right] \\ &\quad + \frac{1}{3}t_1n_1(k),\end{aligned}\quad (13)$$

where $t_j = 8(2\pi)^3 m_\tau m_p \left(\varepsilon_j - \frac{\bar{k}^2}{2\mu_j} \right)$ and $\varepsilon_1 = m_\tau - 2m_p - m_n$, $\varepsilon_3 = m_\tau - m_d - m_p$, $\mu_1 = \frac{(m_p+m_n)m_p}{2m_p+m_n}$ and $\mu_3 = \frac{m_p m_d}{m_p+m_d}$.

In relativistic case mass of the 2N system becomes indefinite. But we have estimated mean squared momentum in the pair $\langle p^2 \rangle$ and find that at $q < 0.7$ GeV/c it is $\langle p^2 \rangle < 0.1$ (GeV/c) 2 . So the effective mass of the pair should be close to the deuteron mass. In the forthcoming calculations we will use such approximation.

Another kind of relativistic effects comes from relativistic deformation of the internal dynamics in the

bound state considered in the infinite momentum frame (IMF). For elastic scattering with rearrangement of clusters, application of the IMF dynamics needs a care, because reaction amplitude can lose symmetry under initial and final states [16]. This problem was also considered in [23] and the appropriate formalism was proposed. Assuming relativistic invariance of the expression

$$\Psi = \frac{\Gamma}{p_{\text{cl}}^2 + m_{\text{cl}}^2} \quad (14)$$

where Ψ is the wave function, Γ is the vertex function for ${}^3\text{He} \rightarrow (np) + p$ virtual decay amplitude, p_{cl} and m_{cl} are the cluster momentum and mass, one can consider the initial and final ${}^3\text{He}$ in their “own IMF”. This infinite momentum frames are defined to be limiting frames in which observer is moved with velocity close to the speed of light in the direction opposite to the motion of the every ${}^3\text{He}$ in the reaction center of mass frame. As a result, the invariance under initial and final states is restored: the wave function for the initial, as well as for the final, ${}^3\text{He}$ will depend on the same light cone variable

$$\alpha = \frac{E_p^* + p^*}{E_\tau^* + p^*}, \quad (15)$$

where the energies E_p^* , E_τ^* and the momentum $p^* = |\vec{p}^*|$ are defined in the reaction center of mass frame.

After that the “relativization procedure” is reduced to the two prescriptions:

- substitute new argument in (13) $k \rightarrow k_{\text{IMF}}$
- change the factor $t_1 \approx t_3 \rightarrow 4(2\pi)^3 \frac{\epsilon_p \epsilon_d (M_{dp}^2 - m_\tau^2)}{(\epsilon_p + \epsilon_d)(1 - \alpha)}$

In these prescription the relativistic internal momentum, k_{IMF} , the invariant mass of virtual $d + p$ pair, M_{dp} , and other variables are expressed as follows:

$$k_{\text{IMF}} = \sqrt{\frac{\lambda(M_{dp}^2, m_d^2, m_p^2)}{4M_{dp}^2}}, \quad (16)$$

$$M_{dp}^2 = \frac{m_p^2}{\alpha} + \frac{m_d^2}{1 - \alpha}, \quad (17)$$

$$\epsilon_p = \sqrt{m_p^2 + k_{\text{IMF}}^2}, \quad \epsilon_d = \sqrt{m_d^2 + k_{\text{IMF}}^2}, \quad (18)$$

where α , defined in (15), is the fraction of the ${}^3\text{He}$ momentum carried by the proton in IMF.

B. High momentum transfer by intermediate pion

The matrix element corresponding to PI-diagram of Figure 1 reads:

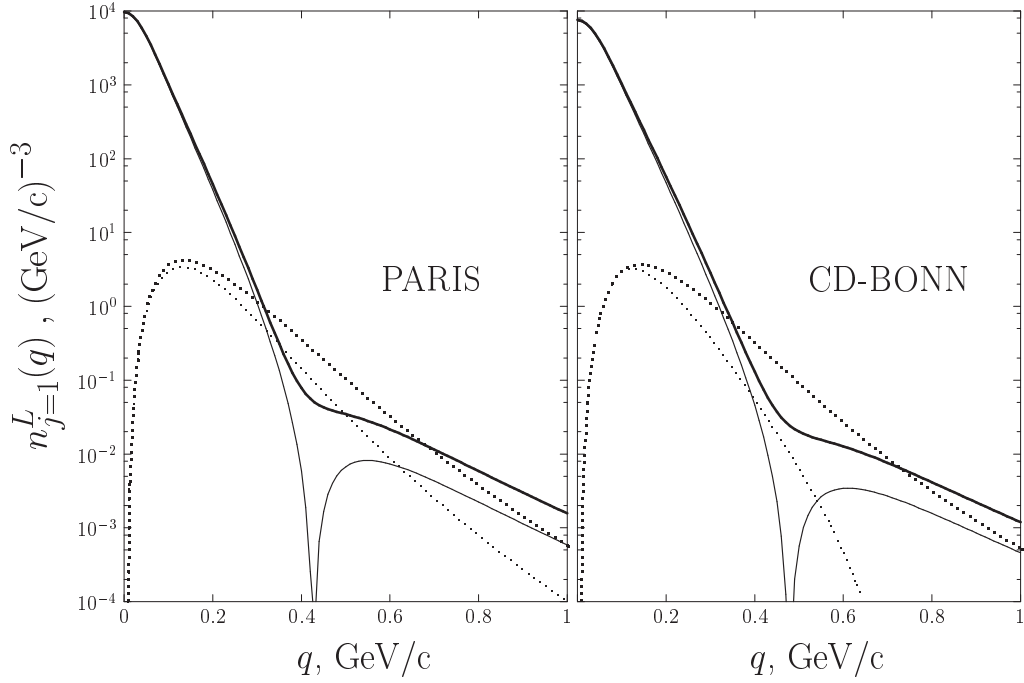


FIG. 2: Momentum distributions of the triplet pair (the full and dotted bold lines are for S and D wave, respectively) and of the the deuteron (the full and dotted thin lines are for S and D wave, respectively).

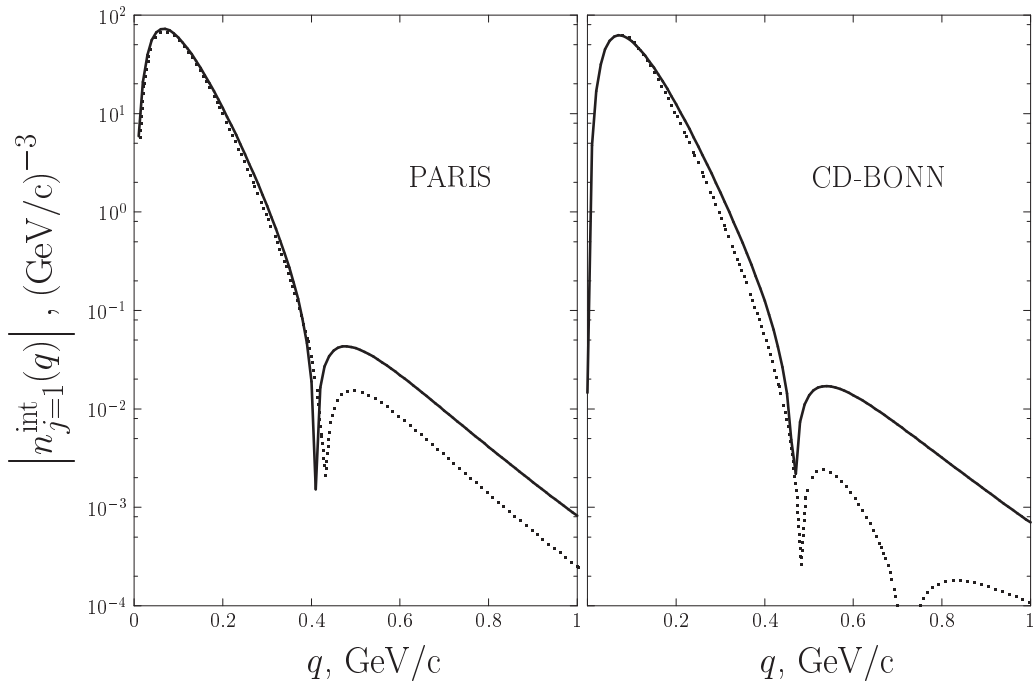


FIG. 3: Interference momentum distribution: the full line is for the triplet pair $n_3^{\text{int}}(q)$ and the dotted line is for $u(q)w(q)$.

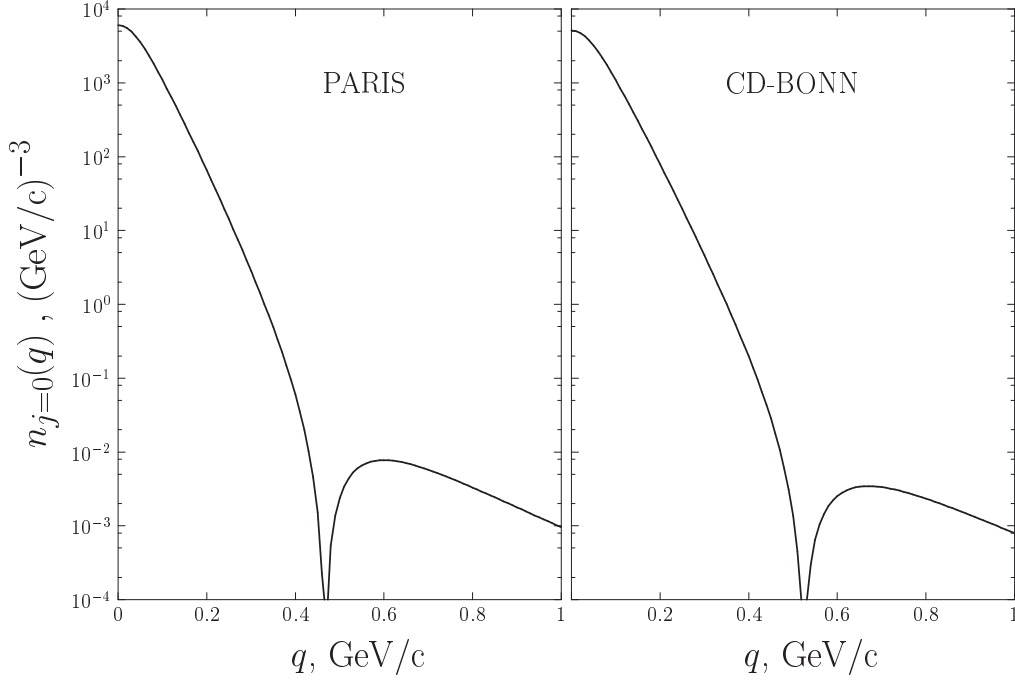
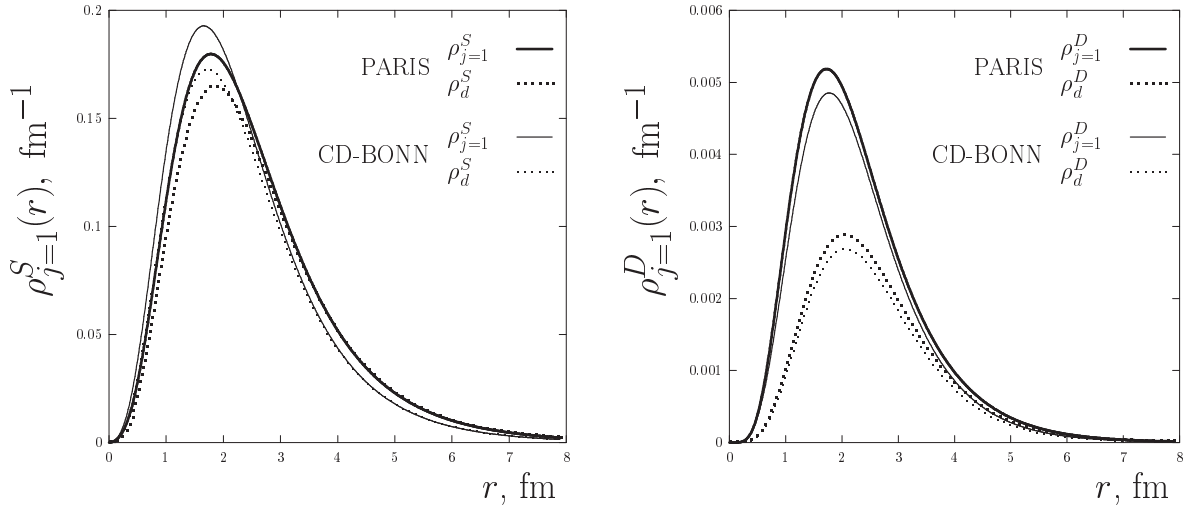


FIG. 4: Momentum distribution of the singlet pair.

FIG. 5: S (left panel) and D (right panel) density for the triplet np pair.

$$\begin{aligned}
\mathcal{M}_{mM}^{m'M'}(\text{PI}) = & -3 \left(\frac{1}{2\pi} \right)^8 \left(2m_p \frac{f_{\pi NN}}{\mu} \right)^2 \int d^4 p_d d^4 p'_d \sum_{\sigma\sigma'} A_{\sigma\sigma'} F_\pi^2(q^2) \bar{u}_{m'}(p') \gamma_5 \frac{1}{\not{p}' - m_p + i0} \Gamma_\mu \varepsilon^\mu(\sigma') U_M(P) \\
& \times \bar{U}_{M'}(P') \Gamma^\nu \varepsilon_\nu^*(\sigma) \frac{1}{\not{p} - m_p + i0} \gamma_5 u_m(p) \frac{1}{(p_d^2 - m_d^2 + i0)(p_d'^2 - m_d^2 + i0)(q^2 - \mu^2 + i0)(q'^2 - \mu^2 + i0)}, \quad (19)
\end{aligned}$$

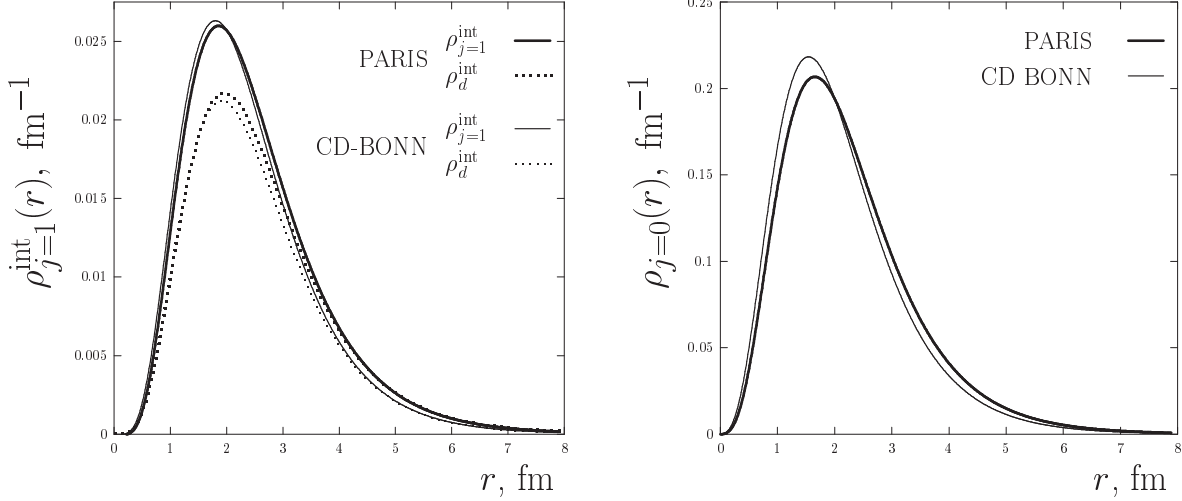


FIG. 6: Interference density for the triplet np pair (left panel) and density for the singlet np pair (right panel).

where $A_{\sigma\sigma'}$ is an amplitude of the subprocess $\pi^0 d \rightarrow \pi^0 d$, μ is the pion mass, $F_\pi(q^2)$ and $f_{\pi NN}$ are the form factor and coupling constant of the πNN vertex. In (19) Γ_μ is the virtual ${}^3\text{He} \rightarrow d + p$ decay amplitude

$$\frac{\bar{u}_m(p)\Gamma_\mu\varepsilon^\mu(\sigma)U_M(P)}{p^2 - m_p^2 + i0} = (2\pi)^{\frac{3}{2}}\sqrt{2m_d}\psi_M^{\sigma m}(\vec{k}). \quad (20)$$

Here and later on we use the following notations: p, P are momenta and m, σ, M are magnetic quantum numbers of the proton, the deuteron and ${}^3\text{He}$, respectively; $\vec{k} = \frac{2}{3}\vec{P} - \vec{p}_d$ is the relative momentum between the proton and the deuteron in ${}^3\text{He}$; ε_3 and μ_3 were already defined in Sec. IV A; $\varepsilon^\mu(\sigma)$ is the polarization vector of the deuteron, $u_m(p)$ and $U_M(P)$ are spinors for the proton and ${}^3\text{He}$; $\psi_M^{\sigma m}(\vec{k})$ is the overlap between the ${}^3\text{He}$ and $p + d$ wave functions. The spinors are normalized as $\bar{u}_m(p)u_{m'}(p) = 2m_p\delta_{mm'}$, etc.

Integrating over the deuteron energies one gets

$$\begin{aligned} \mathcal{M}_{mM}^{m'M'}(\text{PI}) = & 3 \left(\frac{1}{2\pi}\right)^6 \left(2m_p \frac{f_{\pi NN}}{\mu}\right)^2 2m_d(2\pi)^3 \int \frac{d^3 p_d}{2E_d} \frac{d^3 p'_d}{2E'_d} \sum_{\sigma\sigma'} A_{\sigma\sigma'} F_\pi^2(q^2) \chi_{m'}^\dagger \vec{Q}' \vec{\sigma} \chi_{\tilde{m}'} \chi_m^\dagger \vec{Q} \vec{\sigma} \chi_m \\ & \times \frac{\psi_{M'}^{*\sigma\tilde{m}}(\vec{k}') \psi_M^{\sigma'm'}(\vec{k})}{(q^2 - \mu^2 + i0)(q'^2 - \mu^2 + i0)}, \end{aligned} \quad (21)$$

where $\chi_{m(m')}$ and $\chi_{\tilde{m}(\tilde{m}'')}$ are Pauli spinors for the protons, $\vec{Q} = \sqrt{\frac{E_p+m_p}{E_l+m_p}}\vec{l} - \sqrt{\frac{E_l+m_p}{E_p+m_p}}\vec{p}$, $\vec{Q}' = \sqrt{\frac{E_{p'}+m_p}{E_{l'}+m_p}}\vec{l}' - \sqrt{\frac{E_{l'}+m_p}{E_{p'}+m_p}}\vec{p}'$ and $E_d = \sqrt{\vec{p}_d^2 + m_d^2}$, $E'_d = \sqrt{\vec{p}'_d^2 + m_d^2}$.

To simplify the loop integration we take out of the integral the amplitude $A_{\sigma\sigma'}$ and the form factors $F_\pi^2(q^2)$ at

point where the deuteron carries $\frac{2}{3}$ of the ${}^3\text{He}$ momentum. To take into account Fermi motion of the deuteron in ${}^3\text{He}$, these factors were averaged over Gaussian distribution with $\langle p_d^2 \rangle^{1/2} = 41.3$ MeV/c. The latter value was taken from the calculated deuteron momentum distribution in ${}^3\text{He}$. Finally one gets:

$$\mathcal{M}_{mM}^{m'M'}(\text{PI}) = \frac{6}{m_d(2\pi)^3} \left(2m_p \frac{f_{\pi NN}}{\mu}\right)^2 \sum_{\sigma\sigma'} \langle A_{\sigma\sigma'} F_\pi^2 \rangle \chi_{m'}^\dagger \sigma_j \chi_{\tilde{m}'} \chi_m^\dagger \sigma_i \chi_m \mathcal{Q}_{jM}^{\sigma\tilde{m}} \mathcal{Q}_{iM}^{\sigma'm'}, \quad (22)$$

$$\mathcal{Q}_{jM}^{\sigma\tilde{m}} = \int \frac{d^3 p_d Q_j \psi_{M'}^{*\sigma\tilde{m}}(\vec{k})}{2(q^2 - \mu^2 + i0)}, \quad \mathcal{Q}_{iM}^{\sigma'm'} = \int \frac{d^3 p'_d Q'_i \psi_M^{\sigma'm'}(\vec{k}')}{2(q'^2 - \mu^2 + i0)}, \quad (23)$$

$$\langle A_{\sigma\sigma'} F_\pi^2 \rangle = \frac{1}{\sqrt{\pi \langle p_d^2 \rangle}} \int_{-\infty}^{\infty} d\tilde{p} e^{-\frac{(\tilde{p}-p^*)^2}{\langle p_d^2 \rangle}} A_{\sigma\sigma'}(\tilde{s}_{\pi d}, 180^\circ) F_\pi^2(\tilde{q}^2). \quad (24)$$

Now there are two independent three-dimensional integrals and in the nonrelativistic limit the integration over angles can be done analytically.

C. Direct mechanism in optimal approximation

For DIR mechanism we use optimal approximation which minimizes the binding energy and recoil corrections [18]:

$$\mathcal{M}_{mM}^{m'M'}(\text{DIR}) = 3 \sum_{\sigma, m_1, m_1'} M_{mm_1}^{m'm_1'} \times \sum_{\nu\nu'} \int d^3p d^3q \Psi_{M'\sigma m_1'}^{\nu\nu*}(\vec{p}, \vec{q}') \Psi_{M\sigma m_1}^{\nu}(\vec{p}, \vec{q}). \quad (25)$$

The meaning of the quantum numbers M, σ, m etc. is clear from the DIR diagram (Figure 1). The amplitude $M_{mm_1}^{m'm_1'}$ is the on-shell pp elastic scattering amplitude at effective energy, $M_{mm_1}^{m'm_1'}(E_{\text{eff}}, \theta)$, where E_{eff} corresponds to such total energy in the Breit frame as if the struck proton takes all the momentum of ${}^3\text{He}$ [18].

At $\theta_{cm} = 180^\circ$ the pp -amplitude has three independent spin amplitudes [27]:

$$M_{mm_1}^{m'm_1'} = \begin{pmatrix} (a+d) & 0 & 0 & 0 \\ 0 & (a-c) & (a-b) & 0 \\ 0 & (a-b) & (a-c) & 0 \\ 0 & 0 & 0 & (a+d) \end{pmatrix}, \quad (26)$$

with the constraint $a(\pi) - b(\pi) = c(\pi) - d(\pi)$.

Thus in the optimal approximation DIR amplitudes read:

$$\begin{aligned} A^{\text{DIR}} &= \left(a + \frac{d-2c}{3} \right) F_0(p) + \frac{c+d}{3} F_2(p), \\ F^{\text{DIR}} &= \left(a + \frac{2d-c}{3} \right) F_0(p) - \frac{c+d}{3} F_2(p), \\ G^{\text{DIR}} &= -\frac{a-b}{3} [F_0(p) + F_2(p)], \end{aligned} \quad (27)$$

where

$$\begin{aligned} F_0(p) &= 3 \int_0^\infty dr j_0(pr) [u^2(r) + w^2(r)], \\ F_2(p) &= 3 \int_0^\infty dr j_2(pr) [w^2(r) + 2\sqrt{2}u(r)w(r)] \end{aligned} \quad (28)$$

and $p = \frac{2}{3}q$, $q^2 = -(p-p')^2$.

Note that at high energy $a \simeq c$ and $d \simeq b \simeq 0$ so that

$$\begin{aligned} A^{\text{DIR}} &= \frac{a}{3} [F_0(p) + F_2(p)], \\ F^{\text{DIR}} &= \frac{a}{3} [2F_0(p) - F_2(p)], \\ G^{\text{DIR}} &= -A^{\text{DIR}} \end{aligned} \quad (29)$$

For the pp elastic scattering amplitudes a, b, c and d at $E_{\text{eff}} \leq 1300$ MeV we have used results of the partial

wave analysis by Saclay-Geneva group [27]. At higher energy the "diffractive" parametrization was used: $a = c = \frac{p^*}{4\pi}(i + \rho_{pp})\sigma_{pp}^{\text{tot}}$, $d = b = 0$, where ρ_{pp} is the ratio of the real to imaginary part of the forward scattering amplitude and σ_{pp}^{tot} is the total cross section of the pp -scattering.

V. NUMERICAL CALCULATIONS, COMPARISON WITH EXPERIMENT AND PREDICTIONS

The standard parametrization of the form factor $F_\pi(q^2) = (\Lambda^2 - \mu^2)/(\Lambda^2 - q^2)$ with $\Lambda = 1300$ MeV and $f_{\pi NN}^2/4\pi = 0.08$ [24] was used. We have also provided calculations with another cutoff parameter Λ , varying it from 600 to 1700 MeV, but the results were not changed significantly.

Amplitudes $A_{\sigma\sigma'}$ are taken from the partial wave analysis by Virginia group [15]. It must be emphasized here, that in most of the previous studies (see [9, 11, 12, 13, 25, 26]) people either built special theoretical models for the subprocess or made simplifying approximations to replace the amplitude by experimental data on the corresponding cross sections. It is proved by experience that such procedures are not satisfactory.

Results of the calculations at $T_p < 700$ MeV are shown in Figure 7. At the left panel we compare our results with experimental data for the differential cross section. Predictions for the polarization correlation C_{00nn} are given in the right panel of Figure 7. DIR mechanism gives sizable contribution only at high energy ($T_p > 1$ GeV).

VI. CONCLUSIONS AND REMARKS

The main results of this work can be summarized as follows:

- The theoretical description of the proton- ${}^3\text{He}$ EBS at $T_p < 700$ MeV is given. The energy dependence of the differential cross section is described and the polarization correlation C_{00nn} is calculated. The model predicts a structure in energy dependence of the differential cross section and spin-dependent observables between 200 and 400 MeV, which comes from the interference between 2N-exchange and PI-mechanism. Its verification in experiment is now possible and important for understanding mechanism of EBS on the lightest nuclei. Such experimental program is now in preparation in RCNP.
- Only at low energy ($T_p \lesssim 150$ MeV) a cluster two-body approximation $d+p$ for ${}^3\text{He}$ can be justified (see difference between full and dotted curves in Figure 7). At higher energy total three-body structure of ${}^3\text{He}$, including scattering state in triplet and singlet 2N pair, becomes of great importance.

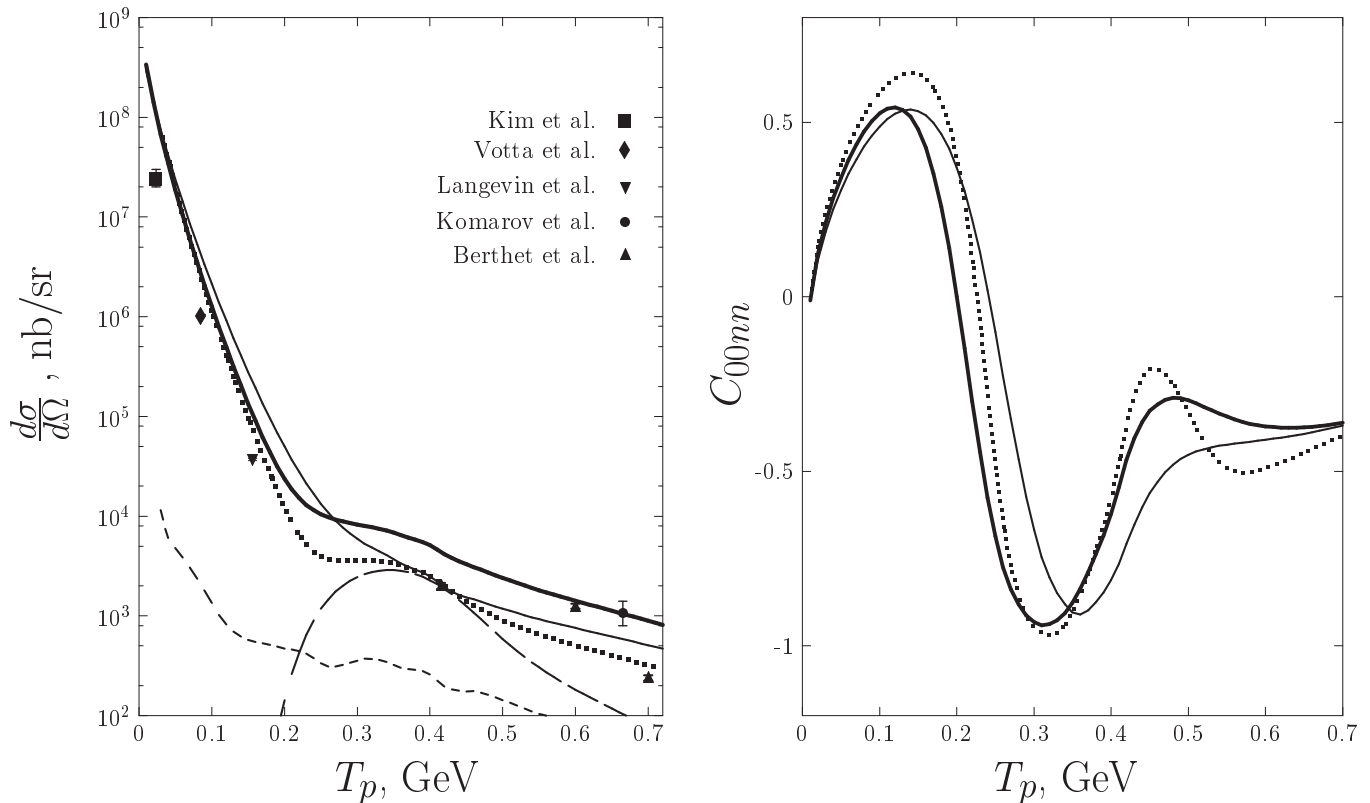


FIG. 7: The differential cross section (left panel) and polarization correlation C_{00nn} (right panel) of the elastic proton- ^3He scattering at $\theta_{c.m.} = 180^\circ$. The solid curves include $(np)_1 + (np)_3$ exchange together with PI-mechanism (the bold and thin curves are for Paris and CD-Bonn potentials, respectively). The one-deuteron-exchange together with DIR and PI mechanisms is shown by dotted line, the contribution of PI and DIR mechanisms in the differential cross section is shown by the long- and short-dashed line, respectively; both are for Paris potential. Data are from [28]-[32]. Data [28]-[30] were extrapolated to $\theta_{c.m.} = 180^\circ$ by us. The point [31] is at $\theta_{c.m.} = 169^\circ$.

- At $T_p \gtrsim 700$ MeV additional mechanisms should be taken into account. Between them one can mention DIR-mechanism and sequential transfer of noninteracting np pair [33]. The later is defined by high relative momentum in the pair, $p > 600$ MeV/c, and low spectator momentum $q \sim 100$ MeV/c. Such high internal momentum in the pair corresponds to a picture of overlapping nucleons and ^3He should be considered rather as a 9-quark system, than a trinucleon bound state.

We do not consider distortion effects in this paper. Such effects were estimated on the basis of Glauber-Sitenko theory [9], but application of such approach at the RCNP energy (as it was done in the recent paper [10]) is very doubtful. This problem, as well as angular dependence of the reaction observables, will be considered in our forthcoming publication.

Acknowledgments

The authors would like to thank M. Tanifuji and H. Toki for stimulating discussions. One of us (A.P.K.) is grateful to A. Boudard for sending the numerical cross section data obtained at SATURNE. We also indebted to F. Lehar for valuable discussion of the partial wave analysis of the pp elastic amplitude by Saclay-Geneva group and for the numerical tables of the partial waves. The authors are thankful to I.I. Strakovsky for a lot of useful discussions of the results of partial wave analysis by Virginia group. Two of the authors (A.P.K., E.A.S.) acknowledge the hospitality of RCNP, where this work was carried out with a Center of Excellence grant from the Ministry of Education, Culture, Sports, Science and Technology (Monbu-Kagaku-sho), Japan.

-
- [1] V.G. Ableev et al., Pis'ma ZhETF 37 (1983) 196 [JETP Lett. 37 (1983) 233]; Nucl. Phys. A393 (1983) 491, A411 541(E); Pis'ma ZhETF 45 (1987) 467 [JETP Lett. 45 (1987) 596]; JINR Rapid Comm. 1[52]-92 (1992) 10; Few Body Systems 8 (1990) 137; C.F. Perdrisat et al., Phys. Rev. Lett 59 (1987) 2840; V. Punjabi et al., Phys. Rev. C39 (1989) 608.
- [2] L.S. Azhgirey et al., Yad. Fiz. 61 (1998) 494 [Phys. At. Nucl. 61 (1998) 432]; V. Punjabi et al., Phys. Lett. B350 (1995) 178.
- [3] I. Sick, Progress in Particle and Nuclear Physics 47 (2001) 245; A.P. Kobushkin and Ya.D. Krivenko, nucl-th/0112009.
- [4] T. Uesaka et al., Nucl. Instr. Meth. A402 (1998) 212.
- [5] K. Hatanaka et al., Study of the $\vec{p}+{}^3\text{He}$ elastic backward scattering at 200—400 MeV. Proposal of experiment 180, 2002, RCNP, Osaka University, Osaka, Japan.
- [6] H. Leśniak and L. Leśniak, Acta Phys. Pol. B9 (1978) 419.
- [7] A.P. Kobushkin, In: Proc. Int. Conf. DEUTERON-93, ed. V.K. Lukyanov (Dubna, 14-18 Sept., 1993) p.71.
- [8] P. Berthet et al., Phys. Lett. 106B (1981) 465.
- [9] Yu.N. Uzikov, Nucl. Phys. A644 (1998) 321.
- [10] Yu.N. Uzikov and J. Haidenbauer, nucl-th/0212092.
- [11] N.S. Cragie and C. Wilkin, Nucl. Phys. B14 (1969) 477.
- [12] V.M. Kolybasov and N.Ya. Smorodinskaya, Phys. Lett. B37 (1971) 272; Yad. Fiz. 17 (1973) 1211 [Sov. J. Nucl. Phys. 17 (1973) 630].
- [13] A. Nakamura and L. Satta, Nucl. Phys. A445 (1985) 706.
- [14] J.C. Anjos, A. Santoro, F.R.A. Simao and D. Levy, Nucl. Phys. A356 (1981) 383.
- [15] R.A. Arndt, I.I. Strakovsky and R.L. Workman, Phys. Rev. C50 (1994) 1796.
- [16] L.A. Kondratyuk et al. Yad. Fiz. 33 (1981) 1208.
- [17] H. Garsilazo and T. Mitsutani, πNN Systems (World Scientific, Singapore, 1990).
- [18] S.A. Gurvitz, J.-P. Dedonder and R.D. Amado, Phys. Rev. C19 (1979) 142; S.A. Gurvitz, Phys. Rev. C20 (1979) 1256.
- [19] V. Baru, J. Haidenbauer, C. Hanhart, and J.A. Niskanen, nucl-th/0207040.
- [20] M. Lacombe et al., Phys. Rev. C 21 (1980) 861.
- [21] R. Machleidt, Phys. Rev. C 63 (2001) 024001.
- [22] R. Schiavilla, V.R. Pandharipande and R.B. Wiringa, Nucl. Phys. A449 (1986) 219.
- [23] A.P. Kobushkin, J. Phys. G 12 (1986) 487.
- [24] R. Machleidt, K. Holinde and Ch. Elster, Phys. Rep. 149 (1981) 1.
- [25] G.W. Barry, Phys. Rev. D7 (1973) 1441.
- [26] L.A. Kondratyuk and F.M. Lev, Yad. Fiz. 26 (1977) 294 [Sov. J. Nucl.Phys. 26 (1977) 153].
- [27] J. Bystricky, F. Lehar and P.Winternitz, J. Physique (Paris) 39 (1978) 1; F. Lehar, private communication.
- [28] C.C. Kim et al., Nucl. Phys. 58, (1964) 32.
- [29] L.G. Votta et al., Phys. Rev. C10 (1974) 520.
- [30] H. Langevin-Joliot et al., Nucl. Phys. A158 (1970) 309.
- [31] V.I. Komarov, G.E. Kosarev and O.V. Savchenko, Sov. J. Nucl. Phys. 11 (1970), 399.
- [32] R. Frascaria et al., Phys. Lett. 66B (1977) 329.
- [33] L.D. Blokhintsev, A.V. Lado and Yu.N. Uzikov, Nucl. Phys. A 597 (1996) 487.